Synthesis of reticulated hollow spheres structure $NiCo_2S_4$ and its application in organophosphate pesticides biosensor

Lei Peng, Sheying Dong, Wenbo Wei, Xiaojing Yuan, Tinglin Huang

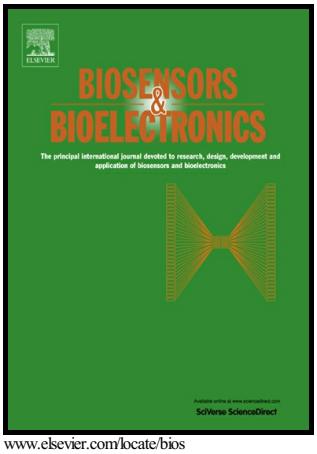

www.elsevier.com/locate/bios

PII: S0956-5663(16)31077-6
DOI: http://dx.doi.org/10.1016/j.bios.2016.10.059
Reference: BIOS9281

To appear in: *Biosensors and Bioelectronic*

Received date: 23 August 2016
Revised date: 13 October 2016
Accepted date: 21 October 2016

Cite this article as: Lei Peng, Sheying Dong, Wenbo Wei, Xiaojing Yuan and Tinglin Huang, Synthesis of reticulated hollow spheres structure $NiCo_2S_4$ and it application in organophosphate pesticides biosensor, *Biosensors an Bioelectronic,* http://dx.doi.org/10.1016/j.bios.2016.10.059

Synthesis of reticulated hollow spheres structure $NiCo_2S_4$ and its application in organophosphate pesticides biosensor

Lei Peng[a], Sheying Dong[a, b]*, Wenbo Wei[b], Xiaojing Yuan[b], Tinglin Huang[a]

[a]*School of Environmental and Municipal Engineering, Xi'an University of Architecture and Technology, Xi'an 710055, China*

[b]*College of Sciences, Xi'an University of Architecture and Technology, Xi'an 710055, China*

*Corresponding author. Tel.: +86 29 82201203; fax: +86 29 82205332.

E-mail address: dongsyy@126.com

Abstract

Electrode materials play a key role in the development of electrochemical sensors, particularly enzyme-based biosensors. Here, a novel $NiCo_2S_4$ with reticulated hollow spheres assembled from rod-like structures was prepared by a one-pot solvothermal method and its formation mechanism was discussed. Moreover, comparison of $NiCo_2S_4$ materials from different experiment conditions as biosensors was investigated by electrochemical impedance spectroscopy (EIS) and differential pulse voltammetry (DPV), and the best one that was reticulated hollow spheres assembled from rod-like structures $NiCo_2S_4$ has been successfully employed as a matrix of AChE immobilization for the special structure, superior conductivity and rich reaction active sites. When using common two kinds of organophosphate pesticides (OPs) as model analyte, the biosensors demonstrated a wide linear range of 1.0×10^{-12}-1.0×10^{-8} g·mL^{-1} with the detection limit of 4.2×10^{-13} g·mL^{-1} for methyl parathion, and 1.0×10^{-13}-1.0×10^{-10} g·mL^{-1} with the detection limit of 3.5×10^{-14} g·mL^{-1}

for paraoxon, respectively. The proposed biosensors exhibited many advantages such as acceptable stability and low cost, providing a promising tool for analysis of OPs.

Keywords: Synthesis; $NiCo_2S_4$; Sensor; Acetylcholinesterase; Organophosphate pesticides

1. Introduction

Recently, transition metal sulfides have attracted great attention because of their unique physical and chemical properties as well as promising applications in fields of catalysis (Lu et al., 2016), sensing (Xing et al., 2016), optoelectronic devices (Kwon et al., 2015), solar energy cells (Sun et al., 2011), and electrode materials (Wu et al., 2016). In particular, the existed studies have shown that the electronic conductivity of nickel cobaltite ($NiCo_2O_4$) was at least two orders of magnitude higher than nickel oxides and cobalt oxides due to its cooperative contributions from both nickel and cobalt ions (Shen et al., 2015; Tarasevich and Efremov, 1982). And what's more, the substitution of oxygen with sulfur could create a more flexible structure due to the lower electronegativity of sulfur than that of oxygen, preventing the disintegration of the structure by the elongation between layers and making it easy for electrons to transport in the structure (Park et al., 2002; Hu et al., 2014).

Motivated by above these, many researches have focused on the synthesis and application of ternary sulfides. For instance, Zhu *et al*. reported a kind of mesoporous $NiCo_2S_4$ nanoparticles prepared by solvothermal route as remarkable supercapacitor electrode materials which manifest excellent electrochemical performances with

ultrahigh specific capacitance, exceptional rate capability and good cycling stability (Zhu et al., 2015). Wang *et al.* obtained a hydrangea-like $NiCo_2S_4$ hollow microsphere by a one-step hydrothermal method. This $NiCo_2S_4$ was used as an advanced electrocatalyst for both oxygen reduction reaction and evolution reaction, indicating that the $NiCo_2S_4$ loaded air electrode performs a nice electrochemical performance in aqueous metal/air battery (Wang et al., 2011a). In recent studies, four different morphologies $NiCo_2S_4$ were successfully synthesized by employing various solvents for the application in pseudocapacitor electrode materials, and the tube-like $NiCo_2S_4$ exhibited promising capacitive properties with high capacitance and excellent retention (Zhang et al., 2014). However, to our knowledge, in most cases, $NiCo_2S_4$ was synthesized in the absence of surfactants, and there are no reports on electrochemical biosensors based on $NiCo_2S_4$ materials.

Apparently, the morphology and structure of $NiCo_2S_4$ have an important influence on the electrochemical performance of $NiCo_2S_4$ material. Alternatively, $NiCo_2S_4$ can offer rich reaction active sites and high electronic conductivity, which encouraged us to explore its application in electrochemical biosensor. Therefore, it is becoming a growing important issue to prepare a novel structure $NiCo_2S_4$ and extend its application on electrochemical biosensor.

Because of rapid response, simple operation, on-site analysis, high sensitivity and low cost, electrochemical AChE biosensor is employed for organophosphate pesticides (OPs) detection (Ding et al., 2014; Zhao et al., 2015; Schulze et al., 2003). The AChE immobilized on an electrode surface can catalyze the hydrolysis of

acetylthiocholine chloride (ATCl) to produce an electro-active product of thiocholine (TCh), which shows an irreversible oxidation peak at as a marker for pesticide detection (Wang et al., 2011). Among that, the key issue is to search for new materials with good electronic conductivity for the immobilization of AChE. More efforts have been attempted the fabrication of biosensor for detecting OPs based on AChE enzymatic inhibition (Kaur et al., 2015; Cancar et al., 2016). Moreover, nafion (NF) is a proton-conductive, chemically inert, insoluble in water and biocompatible perfluorosulfonate linear polymer, which exhibits excellent film-forming ability, and thus possesses almost ideal properties for preparation of AChE biosensor (Chen et al., 2013a; Zhou et al., 2013). The simultaneous presence of NF can enhance the stability of AChE immobilized on the electrode surface and prevent the leakage of AChE from electrode into the solution.

We herein reported a novel reticulated hollow spheres assembled from rod-like structures $NiCo_2S_4$ obtained by a one-pot solvothermal approach using $Co(oAc)_2$, $Ni(oAc)_2$, and Thioacetamide (TAA) as precursors in ethylene glycol (EG) medium with assist of cetyl trimethyl ammonium bromide (CTAB). The effect of reaction conditions such as sulphur precursor, reaction temperature, reaction time and addition agents amounts on the formation of $NiCo_2S_4$ was studied, and the formation mechanism of $NiCo_2S_4$ was discussed. Furthermore, comparison of $NiCo_2S_4$ materials from different experiment conditions as biosensors was investigated by EIS and DPV, and the best one was homogeneously dispersed in NF and then dropped on the surface of CPE to develop a novel AChE modified electrode for the determination of OPs.

2. Materials and methods

The chemicals, apparatus and electrochemical measurements are described in detail in the supporting information.

2.1. Synthesis of $NiCo_2S_4$

The synthesis of $NiCo_2S_4$ is mainly based on previous report (Liu et al., 2013), but surfactant was added. Firstly, $Co(OAc)_2$ (0.3 mmol) , $Ni(OAc)_2$ (0.15 mmol) and 60 mg of CTAB were dissolved in 40 mL of EG under sonication for 5 min. Then, TAA (0.9 mmol) was introduced into the above mixed solution. After transferring the mixture to an autoclave (50 mL), the solvothermal reaction was followed at 180 °C for 8 h. The resulted product was collected by filtration, washed with plenty of deionized water, and dried at 60 °C overnight. The synthesis procedure is shown in **Scheme. 1A.**

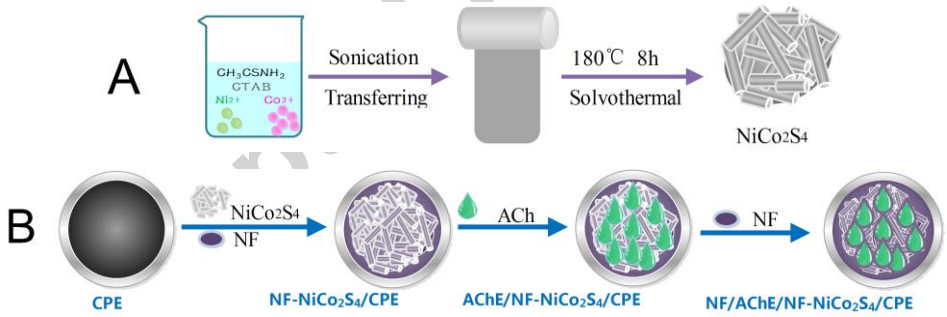

Scheme 1. The illustration of (A) synthesis procedure of $NiCo_2S_4$ and (B) the fabrication process of NF/AChE/NF-$NiCo_2S_4$/CPE

2.2. Preparation of the modified electrodes

CPE was fabricated according to our previous report (Dong et al., 2011), and the detail was described in the Supporting information.

The NF solution (0. 5%, Wt/V) was prepared by diluting 5 % of NF with 0.1 M pH 7.0 PBS. The fabrication process of AChE modified electrode was shown in Scheme. 1B. Firstly, 3 mg of $NiCo_2S_4$ powders and 200 μL 0. 5 % NF solution were dispersed into 800 μL 0.1 M pH 7.0 PBS under sonication for 30 min to obtain homogeneous suspension of NF-$NiCo_2S_4$. Then 6 μL of suspension above was cast onto the surface of a freshly polished CPE to obtain NF-$NiCo_2S_4$/CPE, which was dried at room temperature to form a stable film. Furthermore, AChE/NF-$NiCo_2S_4$/CPE was prepared by casting 6 μL of AChE solution (0.2 $mg \cdot mL^{-1}$) onto NF-$NiCo_2S_4$/CPE. The AChE/NF-$NiCo_2S_4$/CPE modified electrode was dried at 4 °C in a refrigerator and then rinsed with doubly distilled water for twice or thrice to remove the unimmobilized AChE molecules. Finally, the AChE/NF-$NiCo_2S_4$/CPE modified electrode was coated with 5 μl of 0.5 % (Wt/V) NF as the protective membrane to obtain NF/AChE/NF-$NiCo_2S_4$/CPE and stored in 0.1 M pH 7.0 PBS at 4 °C in a refrigerator.

2.3. Detection of pesticides

The NF/AChE/NF-$NiCo_2S_4$/CPE was employed for the determination of pesticides using DPV method. The performance of the biosensor was tested by its DPV response in pH 7.5 PBS solution containing 0.4 mM ATCl. Then the electrode was rinsed with water and incubated in an aqueous solution containing the desired concentration of pesticides (methyl parathion and paraoxon) for 10 min. Finally, it was transferred into the 0.4 mM ATCl solution for DPV measurements at the same condition. The inhibition rate of pesticides was calculated as follows (Eq.1) (Zhao et

al., 2015)

Inhibition (%) = ($i_{p,control}$ - $i_{p,exp}$)/$i_{p,control}$× 1 00% (1)

Where $i_{p,control}$ is the peak current of ATCl on NF/AChE/NF-$NiCo_2S_4$/CPE, $i_{p,exp}$ is the amperometric response of ATCl on NF/AChE/NF-$NiCo_2S_4$/CPE with pesticide inhibition. Inhibition (%) was plotted against the concentrations of the pesticides to obtain linear calibration graphs.

3. Results and discussion

3.1. The characterizations of $NiCo_2S_4$

The morphology of $NiCo_2S_4$ is observed by the scanning electron microscopy (SEM) and transmission electron microscopy (TEM) pattern. Fig. 1A displays a SEM image of the $NiCo_2S_4$, in which many ball-like spheres are seen. From higher magnification SEM images in the inset of Fig.1A, we could further observe these spheres were reticulated and assembled from rod-like structures of relatively uniform with lengths of ～150 nm. To better illustrate the morphology of the as-obtained product, the $NiCo_2S_4$ sample was characterized by TEM (Fig. 1B). It was observed that it is composed of ball-like spheres with hollow structure.

X-ray diffraction (XRD) was employed to characterize the crystal phase of the as-prepared $NiCo_2S_4$. As shown in Fig.1C, we can observe clearly that all the indentified diffraction peaks of samples can be perfectly indexed to cubic phase of $NiCo_2S_4$ (JCPDS card No. 20-0782). The peaks at 26.8°, 31.6°, 38.3°, 50.5°, and 55.3° correspond to the respective (220), (311), (400), (511) and (440) planes of $NiCo_2S_4$, respectively. Element analyses from energy dispersive spectroscopy (EDS)

(Fig.1D) methods verify the presence of S, Co and Ni and their atomic ratio is about 4:2:1. Therefore, the as-prepared material is $NiCo_2S_4$.

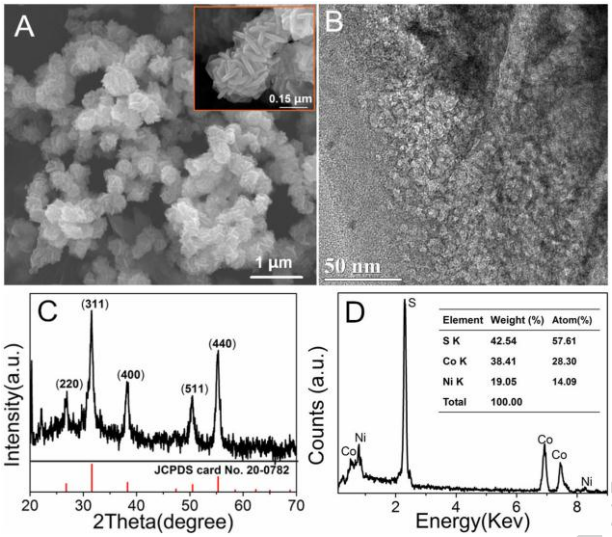

Fig.1. (A) SEM images (B) TEM images (C) XRD pattern (D) EDS spectrum of $NiCo_2S_4$.

3.2. The effect of various conditions on the preparation of $NiCo_2S_4$

To investigate the effects of different sulphur precursor (Fig.2A_1-A_4), reaction temperature (Fig.2B_1-B_4), reaction time (Fig.2C_1-C_4) and addition amounts of CTAB (Fig.2D_1-D_4) on the growth of $NiCo_2S_4$ in synthetic route, parallel experiments were also carried out, the results are shown in Fig. 2 and the detail was described in the Supporting information. From these results, we concluded that the addition amount of CTAB and reaction temperatures played more important roles in the formation of the rod-like structure which was the best one in above $NiCo_2S_4$ materials employed as a matrix of AChE immobilization for the special structure, superior conductivity and rich reaction active sites.

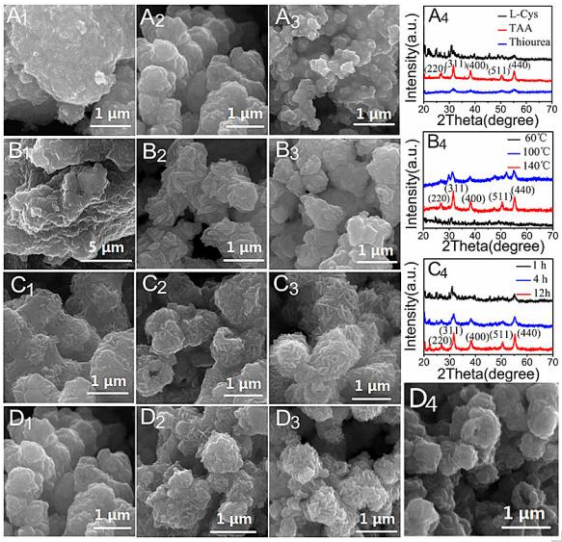

Fig. 2. SEM images of $NiCo_2S_4$ prepared with different sulphur sources（A_1）L-Cys (A_2) TAA（A_3）thiourea, at different reaction temperatures（B_1）60 °C (B_2) 100 °C（B_3）140 °C, in different reaction time（C_1）1 h (C_2) 4 h （C_3）12 h, with different amounts of CTAB (D_1) 0 mg (D_2) 20 mg (D_3) 100 mg (D_4) 200 mg and their XRD patterns(A_4, B_4,C_4).

3.3. Formation mechanism of $NiCo_2S_4$

On the basis of above several experimental results, we propose the following plausible mechanism for the formation of reticulated hollow spheres $NiCo_2S_4$ with rod-like structures. The metal ions and TAA were dispersed in EG to form droplets with assistant of CTAB. With the increasing of temperature, TAA started to decompose and further S^{2-} ions diffused towards to metal ions for the growth of $NiCo_2S_4$ (Yu et al., 2013). Thus, the sulfur sources mainly influenced the growth stage of $NiCo_2S_4$ controlled by the diffusion mechanism. The high temperature is beneficial to the decomposition of TAA and the oriented growth of nuclei of $NiCo_2S_4$ with

rod-like structures. When the temperature is high, the rate of mass transport will be more drastically than the rate of aggregation or deposition. The nuclei will be grown along the low-energy direction on the surface of structures, so the rod-like structures $NiCo_2S_4$ is observed (Bai et al., 2015; Zhao et al., 2008). Following, the S^{2-} ions are much enough to react with metal ions to form the nucleation of the $NiCo_2S_4$, and then it grows as certain direction with assistant of CTAB to generate rod-like structures. In addition, with the passage of time, the rod-like structures continue to grow up and assembled reticulated hollow spheres as well as achieve good crystallinity.

3.4. Electrochemical behavior of the modified electrodes

EIS experiments were done to investigate the effect of the modification process on the impedance of the electrode surface. Electronic transfer resistance (R_{et}) can be determined by calculating the diameter of the high-frequency semicircle in the Nyquist curve (Bard and Faulkner, 1980; Narang et al. 2015; Narang et al. 2016; Singhal, C., et al. 2016). A Nyquist plot of the impedance data fits with the Randles circuit which was illustrated in the inset of Fig. 3A, exhibiting the equivalent circuit used to fit all the EIS experiments in which R_{et} is the electron transfer resistance, R_s is the solution resistance, CPE is the constant phase element, and Z_W is the Warburg element. Keeping other condition of modified CPE constant, the EIS of various $NiCo_2S_4$ materials obtained from varying reaction condition was shown in Fig.3A. Obviously, when the reaction time is 8h, $NiCo_2S_4$/CPE has the lowest R_{et} value, which may be attributed to the excellent electrical conductivity of reticulated hollow spheres $NiCo_2S_4$.

As seen in Fig.3B, when NF and $NiCo_2S_4$ composites were coated on the CPE, it was found that the R_{et} increased comparing with $NiCo_2S_4$/CPE, suggesting that NF had been successfully introduced into $NiCo_2S_4$. After AChE was immobilized on the NF-$NiCo_2S_4$/CPE, the R_{et} of the modified electrode slightly increased, and the R_{et} of AChE/NF-$NiCo_2S_4$/CPE further increased. This is because that the dielectric behavior of enzymes molecules could result in a higher barrier for interfacial electron transfer, demonstrating the fact that AChE had been successfully immobilized on the NF/AChE/NF-$NiCo_2S_4$/CPE. In addition, compared with other structures, the reticulated hollow sphere of smaller size and loose structure has a larger surface area which is more conducive to the subsequent immoblization of enzymes.

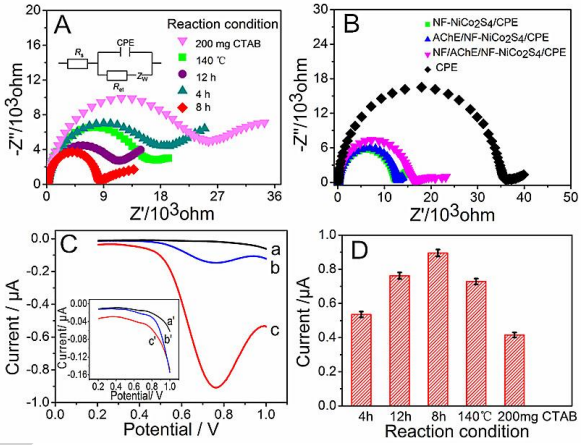

Fig.3. EIS of (A) the obtained $NiCo_2S_4$ from different conditions modified electrodes (B)CPE, NF-$NiCo_2S_4$/CPE, AChE/NF-$NiCo_2S_4$/CPE and NF/AChE/NF-$NiCo_2S_4$/CPE in the solution of 5.0 mM $K_3Fe(CN)_6/K_4Fe(CN)_6$ (1:1) containing 0.1 M KCl. Amplitude: 0.005 V; the frequencies:1 0^5 to 10^{-2} Hz; bias potential: 0.20 V. The inset shows the Randles equivalence circuit for the CPE. (C) DPVs of NF/AChE/CPE(a/a′), NF/AChE/NF/CPE(b/ b′), NF/AChE/NF-$NiCo_2S_4$/CPE and (c/c′) within/without 0.4 mM ATCI in 0.1 M pH 7.5 PBS (D) The current intensity of CPE modified by

$NiCo_2S_4$ obtained from different conditions. Error bars are coefficient of variation across three repetitive experiments.

As shown in Fig.3C, the DPVs of various electrodes were investigated in 0.1 M pH 7.5 PBS. As shown in inset, no oxidation peaks was observed at (a′) NF/AChE/CPE , (b′) NF/AChE/NF/CPE and (c′) NF/AChE/NF-$NiCo_2S_4$/CPE for the lack of electroactive species in the examined range. When 0.4 mM ATCl was added into the PBS, no oxidation peaks was observed at (a) NF/AChE/CPE. In contrast, the peak current increased in different degrees as following order: NF/AChE/NF-$NiCo_2S_4$/CPE >NF/AChE/NF/CPE after the addition of 0.4 mM ATCI.

Furthermore, the current intensity of CPE modified by $NiCo_2S_4$ obtained from different conditions was measured by DPV, and results were shown in Fig.3D. Obviously, NF/AChE/NF-$NiCo_2S_4$/CPE has the biggest current values, which was consistent with results of EIS. Firstly, the enhanced electrochemical response can be ascribed to the good conductivity of $NiCo_2S_4$ due to lower band gap (Chen et al., 2013b), which could effectively promote the electrocatalysis toward TCh. Secondly, the high surface area and more active sites of the reticulated hollow spheres $NiCo_2S_4$ are devoted to the increase of the surface loading of AChE. Besides, NF protective membrane was used to prevent the loss of the enzyme molecules, improve the antiinterference ability of the biosensor and provide a biocompatible microenvironment to maintain enzymatic activity of the AChE.

3.5. Optimization parameters of the biosensor performance

The response currents of the enzyme electrode were investigated in a series of

PBS with 0.1 M pH from 6.0 to 8.0 including 0.4 mM ATCl (Fig. 4A). The maximum value of the response current was at pH 7.5. Thus, a pH 7.5 of PBS was used in the subsequent experiment.

The influence of AChE amount and volume of NF-$NiCo_2S_4$ on the response of biosensor was also investigated (Fig. 4B and Fig. 4C). The results showed that with the increasing of the AChE amount, the peak current increased gradually and reached the maximal value at 0.162 U. After that, the amperometric response decreased gradually as the amount of AChE further increased. During the volume of NF-$NiCo_2S_4$ ranged from 2 μL to 10 μL, the NF/AChE/NF-$NiCo_2S_4$/CPE response increase, and then decrease along with the concentration. Therefore, 0.162 U of AChE and 6 μL of NF-$NiCo_2S_4$ were chosen as the optimal enzyme amount and volume of NF-$NiCo_2S_4$ for preparation of the biosensor.

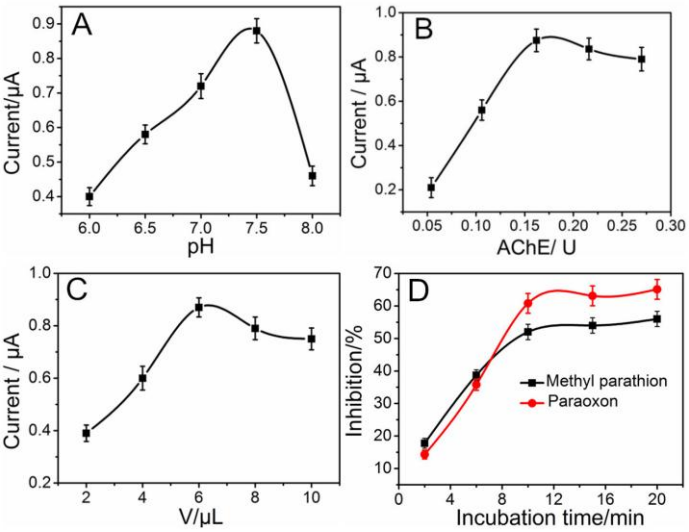

Fig.4. Effect of (A) different pH values (B) AChE amount (C) NF-$NiCo_2S_4$ dosage on response current of the NF/AChE/NF-$NiCo_2S_4$/CPE (D) Inhibition on 10^{-8} g·mL^{-1} methyl parathion and 10^{-10} g·mL^{-1} paraoxon at different incubation time by DPV in 0.4 mM ATCl. Error bars are coefficient of variation across three repetitive

experiments.

In addition, incubation time played a great influence on AChE-based pesticide analysis. The effect of inhibition on AChE activity at different incubation times (2–20 min) was studied separately in 10^{-8} g·mL^{-1} methyl parathion and 10^{-10} g·mL^{-1} paraoxon, respectively. As shown in Fig. 4D, the inhibition increased sharply with the increasing of incubation time before 10 min, but the inhibitions tended to a stable value when further increasing incubation time, indicating the binding interaction between pesticides and active target groups in the enzyme reaches saturation Hence, 10 min was chosen as the optimal incubation time.

3.6. Amperometric response to ATCl

Fig.5A showed a typical current–time plot of CPE (curve a) and NF/AChE/NF-$NiCo_2S_4$/CPE (curve b) without ATCl in 0.1 M pH 7.5 PBS at an applied potential of 800 mV under stirring. There was no obvious change in current response at these electrodes. However, upon addition of an aliquot of ATCl to the PBS buffer, the current reached 95 % of its steady state within 6 s (curve c). The response current increased linearly with the increasing ATCl concentration in two ranges: 0.5-127 μM and 127-477 μM. The egression equations were：i (μA)= -0.00212c(μM) -0.03253（R=0.9916）and i(μA)= -0.000242c (μM)- 0.26029（R=0.9889). The two linear ranges indicated that the linear range of AChE biosensors for acetylcholine was approximately two orders of magnitude. The detection limit of 0.18 μM was obtained at a signal to noise of 3. When the concentration of ATCl was higher than 477 μM, a platform was observed, showing a characteristic of the Michaelis-Menten kinetic

mechanism. The Michaelis-Menten constant (K_M) value for the enzymatic activity of the NF/AChE/NF-$NiCo_2S_4$/CPE to ATCl was estimated with the Lineweaver–Burk equation (Eq.2):

$$1/I_{ss} = 1/I_{max} + K_M /I_{max} \cdot 1/c \quad (2)$$

Where I_{ss} is the steady-state current after the addition of substrate, I_{max} is the maximum current measured under saturated substrate condition, and C is the bulk concentration of the substrate (Wang et al., 2011b). The K_M value was determined by analysis of the slope and intercept for the plot of the reciprocals of the steady-state current versus ATCl concentration. The K_m value was to be 0.076 mM, which is much smaller that of 0.18 mM for AChE/CMC/GCE (Kandimalla and Ju, 2006), 0.16 mM for AChE/CPBA/AuNPs/RGO-CS/GCE (Liu et al., 2011), 0.202 mM for AChE/AuNPs/cr-Gs (Wang et al., 2011b) and 0.131 mM for NF/AChE-CS/ SnO_2-CGR-NF/GCE (Chen et al., 2013a), indicating a higher affinity of the NF/AChE/NF-$NiCo_2S_4$/CPE to ATCl.

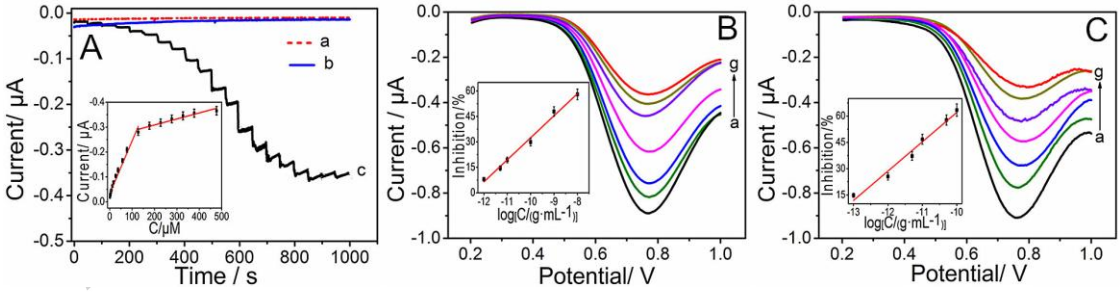

Fig5. (A) Amperometric current-time response curves of (a) CPE and (b) NF/AChE/NF- $NiCo_2S_4$/CPE without ATCl as well as (c) NF/AChE/NF-$NiCo_2S_4$/CPE upon successive addition of ATCl into 0.1M pH 7.5 PBS solution. Applied potential: 0.8V. Inset: calibration curve of steady-state currents vs. the concentration of ATCl at NF/AChE/NF-$NiCo_2S_4$/CPE; DPV response of NF/AChE/NF-$NiCo_2S_4$/CPE in 0.1M

pH 7.5 PBS containing 0.4 mM ATCl after incubation in（B）(a-g): 0, 10^{-12}, 5×10^{-12}, 10^{-11}, 10^{-10}, 10^{-9} and 10^{-8} g·mL^{-1} of methyl parathion (C) (a-g): 0, 10^{-13}, 10^{-12}, 5×10^{-12}, 10^{-11}, 5×10^{-11} and 10^{-10} g·mL^{-1} of paraoxon for 10 min. Insert: Inhibition curve of NF/AChE/NF-$NiCo_2S_4$/CPE biosensor for the determination of methyl parathion or paraoxon by DPV.

3.7. Pesticides determination

The DPV responses were examined before and after exposure to different concentration pesticides. The response of NF/AChE/NF-$NiCo_2S_4$/CPE showed an obvious peak at 760 mV (Fig.5B/C-a) in pH 7.5 PBS containing 0.4 mM ATCl.The peak came from the oxidation of TCh which was hydrolysis product of ATCl catalyzed by immobilized AChE (Du et al., 2007), which was associated with the inhibition of AChE activity based on the amount of pesticide added. The decrease in redox peak current likely occurred as a result of blocking serine hydroxyl groups of AChE by covalently bound of pesticides, which invariably reduced the overall charge of the catalytic active site. As shown in the inset Fig.5B/C, the linear range were found to be 1.0×10^{-12}-1.0×10^{-8} g·mL^{-1} with the detection limit of 4.2×10^{-13} g·mL^{-1} for methyl parathion, 1.0×10^{-13}-1.0×10^{-10} g·mL^{-1} with the detection limit of 3.5×10^{-14} g·mL^{-1} for paraoxon, respectively. Compared with other reported AChE biosensors summarized inTable S1 (Gong et al., 2013; Raghu et al., 2012; Wei et al., Yu et al., 2015; Jha and Ramaprabhu 2010; Liu et al., 2006), the performance of the present NF/AChE/NF-$NiCo_2S_4$/CPE had a wider range, and lower detection limit, indicating that the NF/AChE/NF-$NiCo_2S_4$ film not only improved the electron transfer rate, but

also decreased the detection limit in the quantitative analysis of pesticides. Therefore, NF/AChE/NF-$NiCo_2S_4$/CPE biosensor would be an excellent platform for the detection of pesticides.

The fabrication reproducibility for six NF/AChE/NF-$NiCo_2S_4$/CPE was carried out by comparing their currents in pH 7.5 PBS containing 0.4 mM ATCl. The relative standard deviation (RSD) was 5.3 % (n = 6), revealing an excellent reproducibility of the electrode preparation procedure. In addition, the electrode retained 92 % of its initial peak current response after it was kept in refrigerator at 4 °C in pH 7.5 PBS for two weeks, which shows long-term stability of the NF/AChE/NF-$NiCo_2S_4$/CPE surface.

4. Conclusions

In summary, a novel $NiCo_2S_4$ which was composed of reticulated hollow spheres assembled from rod-like structures was fabricated in the presence of surfactant. The studies of growth status of as-prepared $NiCo_2S_4$ indicated that the reaction temperature and addition amounts of CTAB had more significant influence on its formation. Compared with other $NiCo_2S_4$ materials in this work, the reticulated hollow spheres $NiCo_2S_4$ has the best electrochemical performance and can further be employed as a platform for highly efficient immobilization of AChE on CPE to construct OPs biosensor. Benefiting from high surface area, more active sites and good conductivity of $NiCo_2S_4$, the proposed biosensor exhibits low detection limit, wide linear range and good stability. The study not only prepared a novel $NiCo_2S_4$, but

also extended its application on electrochemical biosensor field.

Acknowledgments

The authors appreciate the support from the National Natural Science Foundation of China (No. 21575111), and the Projects in the National Science & Technology (No. 2012BAC04B02).

References

Bai, W.S., Sheng, Q.L., Nie, F., Zhen, J.B., 2015. ACS Appl. Mater. Inter. 7 (51), 28377-28386.

Bard, A. J., Faulkner, L. R., 1980. Electrochemical Methods: Fundamentals Application, Second ed. Wiley, New York .

Cancar, H.D., Soylemez, S., Akpinar, Y., Kesik, M., Göker, S., Gunbas, G., Volkan, M., Toppare, L., 2016. ACS Appl. Mater. Inter. 8 (12), 8058-8067.

Chen, Z., Xia, S., Zhao, W. P., Gong, Z. L., Wang, X.Y., 2013a. Biosens. Bioelectron. 42, 124-130.

Chen, H.C., Jiang, J.J., Zhang, L., Wan, H. Z., Qi, T., Xia, D. D., 2013b. Nanoscale 5, 8879-8883.

Ding. J., Zhang, H., Jia, F., Qin, W., Du, D., 2014. Sensor. Actuat. B-Chem. 199, 284-290.

Dong, S. Y., Zhang, P. H., Liu, H., Li, N., Huang, T. L., 2011. Biosens. Bioelectron. 26 (10), 4082-4087.

Du, D., Huang, X., Cai, J., Zhang, A.D., 2007. Biosens. Bioelectron. 23 (2), 285-289.

Gong, J.M., Guan, Z. Q., Song, D. D., 2013. Biosens. Bioelectron. 39 (1), 320-323.

Hu. W., Chen. R., Xie, W., Zou, L., Qin, Bao, N. D., 2014. ACS Appl. Mater. Inter. 6 (21), 19318-19326.

Jha, N., Ramaprabhu. S., 2010. Nanoscale 2, 806-810.

Kandimalla, V.B., Ju, H., 2006. Chem. Eur. J. 12 (4), 1074-1080.

Kaur, B., Srivastava, R., 2015. New J. Chem. 39, 6899-6906.

Kwon, K. C., Kim, C., Le, Q. V., Gim, S., Jeon, J. M., Ham, J. Y., Lee, J. L., Jang, H.W., Kim, S. Y., 2015. ACS Nano 9 (4), 4146-4155.

Liu, G.D., Lin, Y.H., 2006. Anal. Chem. 78 (3), 835-843.

Liu, Q., Jin, J.T., Zhang, J. Y., 2013. ACS Appl. Mater. Inter. 5 (11), 5002-5008.

Liu, T., Su, H.C., Qu, X., Ju, P.J., Cui, L., Ai, S.Y., 2011. *Sensor. Actuat. B-Chem.* 160 (1), 1255-1261.

Lu, Q.P., Yu, Y.F., Ma, Q.L., Chen, B., Zhang, H., 2016. Adv. Mater. 28 (10), 1917-1933.

Narang, J., Malhotra, N., Singh, G., Pundir, C.S., 2015. Biosens. Bioelectron. 66, 332-337.

Narang, J., Singhal, C., Malhotra , N.,Narang, M., PN, A.K.,Gupta, R., Kansal, R., Pundir, C.S., 2016. Biosens. Bioelectron. 86, 566-574.

Park, S. H., Sun,Y.K., Park, K.S., Nahm, K.S., Lee, Y.S., Yoshio, M., 2002.

Electrochim. Acta 47 (11), 1721-1726.

Raghu, P., Swamy, BEK., Reddy, T.M., Chandrashekar, B.N., Reddaiah, K., 2012. Bioelectrochemistry 83,19-24.

Schulze, H., Vorlová, S., Villatte, F., Bachmann, T.T., Schmid, R.D., 2003. Biosens. Bioelectron. 18 (2-3), 201-209.

Shen, L. F., Yu, L., Yu, X.Y., Zhang, X.G., Lou, X. W., 2015. Angew. Chem. Int. Ed. 54 (6), 1868-1872.

Singhal, C., Malhotra , M., Pundir, C.S., Deepshikha., Narang, J., 2016. Mat. Sci. and Engg. C. 69, 769-779.

Sun, H.C., Qin, D., Huang, S.Q., Guo, X. Z., Li, D. M., Luo, Y. H., Meng, Q. B., 2011. Energ. Environ. Sci. 4, 2630-2637.

Tarasevich, M. R., Efremov, B. N., 1982. Electrodes of Conductive Metallic Oxides, Part A (Ed: S. Trasatti), Elsevier, USA.

Wang, K., Liu, Q., Dai, L., Yan, J. J., Ju, C., Qiu, B. J., Wu, X. Y., 2011a. Anal. Chim. Atca 695 (1-2), 84-88.

Wang, M.R., Lai, Y. Q., Fang, J., Qin, F. R., Zhang, Z., Li, J., Zhang, K., 2016. Catal. Sci. Technol. 6, 434-437.

Wang, Y., Zhang, S., Du, D., Shao, Y., Li, Z., Wang, J., Engelhard, M. H., Li, J., Lin, Y., 2011b. J. Mater. Chem. 21, 5319-5325.

Wei, M., Zeng, G. Y., Lu, Q. Y., 2014. Microchim Acta 181, 121-127.

Wu, C., Maier, J., Yu, Y., 2016. Adv. Mater. 28 (1), 174-180.

Xing, Z. C., Wang, L., Yang, X. R., 2016. J. Mater. Chem. B. 4, 2860-2863.

Yu, G. X., Wu, W.X., Zhao, Q., Wei, X.Y., Lu, Q., 2015. Biosens. Bioelectron. 68, 288-294.

Yu, L., Zhang, L., Wu, H. B., Lou, X. W., 2014. Angew. Chem. Int. Ed. 53 (14), 3711-3714.

Zhang, Y. F., Ma, M. Z., Yang, J., Sun, C. C., Su, H. Q., Huang, W., Dong, X. C., 2014. Nanoscale 6, 9824-9830.

Zhao, H. Y., Ji, X. P., Wang, B. B., Wang, N., Li, X.R., Ni, R.X., Ren, J.J., 2015. Biosens. Bioelectron. 65, 23-30.

Zhao, P.T., Huan, K.X., 2008. Cryst. Growth Des. 8 (2), 717-722.

Zhou, Q., Yang, L., Wang, G., Yang, Y., 2013. Biosens. Bioelectron. 49, 25-31.

Zhu, Y.R., Wu, Z. B., Jing, M. J., Yang, X. M., Song, W. X., Ji, X. B., 2015. J. Power Sources 273, 584-590.

Graphical Abstract

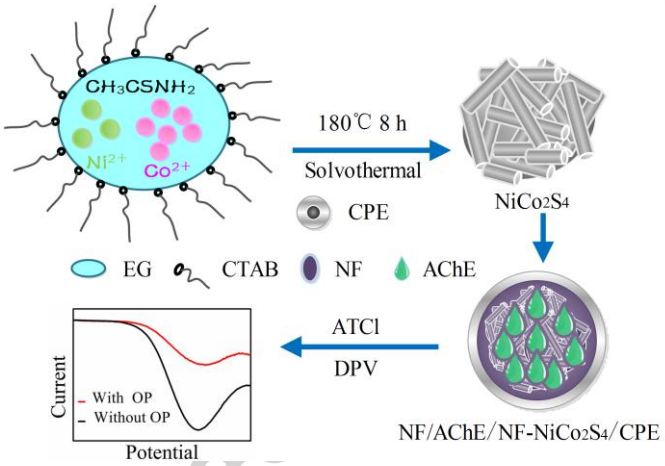

Highlights

- Novel structure $NiCo_2S_4$ with reticulated hollow spheres was fabricated by a hydrothermal method.
- The formation mechanism of the obtained $NiCo_2S_4$ was discussed.
- The preparation of organophosphate pesticides biosensor based on NF-$NiCo_2S_4$ was simple and convenient.